Analysis of Atmospheric Pressure Plasma Parameters During Treatment of Polyethylene Terephthalate Films

Thorsten Deichmann,[1] Marian G. McCord,[2] Mohamed A. Bourham,[3] Thomas Gries[1]

[1]*Institut für Textiltechnik, RWTH Aachen University, Aachen, Germany*
[2]*Department of Textile Engineering, Chemistry and Science, North Carolina State University, Raleigh, North Carolina*
[3]*Department of Nuclear Engineering, North Carolina State University, Raleigh, North Carolina*

Received 29 April 2010; accepted 7 October 2010
DOI 10.1002/app.33557
Published online 10 March 2011 in Wiley Online Library (wileyonlinelibrary.com).

ABSTRACT: The North Carolina atmospheric plasma system (NCAPS) was interfaced with electric diagnostics and computer-based instrument control hardware and software to display plasma parameters in real-time. The monitoring system is also interfaced with gas flow controllers and a Teflon-coated thermocouple for continuous monitoring of the gas flow and the ambient temperature inside the plasma test cell. A simplified plasma model was developed and built in the interface system to solve for the plasma electron number density and display the results during device operation. Polyethylene terephthalate (PET) films were treated in the device using various gas combinations. The ambient gas temperature inside the test cell increases from 83 to close to 95°F (28.33–35°C) for most gases within 30 s, and further increases to about 105 (40.6°C) after 300 s of operation, indicating a nonthermal plasma condition inside the test cell. The interface solver shows that the electron number density decreases when PET films are immersed in the plasma, indicating recombination of etched species to the free electrons. Contact angle measurements showed that the wettability of PET surfaces increased after plasma exposure for all used gas combinations. Measurements of Young's modulus with dynamic mechanical analysis (DMA) showed an increase of the modulus of PET after treatment with helium plasma, whereas the modulus slightly decreased after treatment with oxygen, tetrafluorocarbon and hexafluorocarbon gases. © 2011 Wiley Periodicals, Inc. J Appl Polym Sci 121: 1875–1884, 2011

Key words: atmospheric plasma; cold plasma; polyesters; films; modeling

INTRODUCTION

Polyethylene terephthalate (PET) is a well-characterized thermoplastic polymer that is frequently used for medical applications including artificial vascular grafts, sutures, and meshes. In addition, PET can be converted by conventional techniques into molded articles such as luer filters, check valves, and catheter housings.[1] PET can also be used in synthesis of implant materials that can be biointegrated into native tissue, which is a desired outcome for indwelling permanent devices. Such implants must have improved biocompatibility (chemical composition, wettability, surface energy, surface charge, etc.) to denature neighboring proteins. Improved biocompatibility may be achieved via chemical or physical surface modification.[2] Several different approaches have been used to give vascular PET grafts an antithrombogenic luminal surface that would increase the patency of small internal diameter (<6 mm) grafts.[1–5] Occlusion problems still exist due to nonuniform cell coverage of the whole prosthetic surface. It has been shown that endothelial cell adhesion on PET polymer is poor,[6,7] hence optimizing the chemistry of the polymer surface is required. Modifying PET to provide improved surface properties and functionalities is important to satisfy, and expand on, medical applications. Surface modification may be achieved by several wet-chemistry methods; however, the successful evolution in atmospheric pressure plasma methods is becoming a versatile tool for modifying textiles surface chemistries that improve the wettability, adhesion, and biocompatibility by introducing functional groups or depositing thin films of defined compositions or grafting compounds of special features such as antimicrobials and slow-release of pharmaceuticals. Plasma treatment has proven to be an effective method for altering surface properties without adversely affecting bulk properties including strength and toughness; however, this caveat is not always valid for high surface to volume ratio materials like thin films and fibers, where the surface and bulk may be indistinguishable. This research focuses on investigation of atmospheric plasma surface modification of PET in an atmospheric pressure dielectric

Correspondence to: M. G. McCord (marian_mccord@ncsu.edu).

barrier discharge plasma device in which plasma parameters, electron number density, and ambient gas temperature, are continuously monitored via a computer interface system with a mathematical solver for a simplified plasma electric circuit equivalent model.

The North Carolina Atmospheric Plasma System (NCAPS) is housed in the College of Textiles at North Carolina State University; it is a custom-built pilot scale capacitively-coupled atmospheric pressure dielectric-barrier discharge designed to provide batch treatment of textiles and biomaterials, as well as continuous treatment of fabrics.[8,9] Computer-based instrument control hardware and software were interfaced with plasma diagnostics to monitor plasma parameters, specifically plasma electron number density, and operating conditions during the plasma treatment process, which provides continuous monitoring of discharge voltage and current, frequency, gas flow rates, and the ambient temperature inside the plasma chamber. A mathematical solver was integrated inside the software to calculate the representative plasma parameters, plasma impedance, the electron number density, and electron kinetic temperature in real time. PET films were treated with four different plasma gases with helium as the seed gas, and other gases are added at 1% by volume (He; He + 1%O_2; He + 1%CF_4; He + 1%O_2 + 1%CF_4). The treated films were characterized by weight loss, contact angle measurement, and dynamic mechanical analysis (DMA).

EXPERIMENTAL

Atmospheric plasma facility (NCAPS)

The atmospheric pressure plasma device, NCAPS, operating at 760 Torr, is a capacitively-coupled dielectric barrier discharge (DBD) operated by a 4.8 kW audio frequency power supply at 4–10 kHz.[8,9] Two transformers 180° out of phase coupled to the power supply provide the high voltage to the electrodes. The device has an active exposure area of $\sim 60 \times 60$ cm^2 between two copper electrodes with each electrode embedded inside of a Lexan® polycarbonate insulator, with a fixed 5-cm gap separation; however, the system has the capability to operate at up to 8-cm gap separation. Helium gas is used as the seed gas to initiate the discharge and is injected between the electrodes into the test cell at a constant flow rate of ~ 10 L min^{-1}. Depending on the desired treatment, other gases such as oxygen, argon, nitrogen, hydrogen, CF_4, C_3F_6, forming gas (90% N_2 + 10%H_2), CH_4, CO_2, could be added at a specific flow rate into the test cell. The dielectric-barrier discharge is a nonequilibrium discharge generates low-temperature (0.5–1.2 eV), low electron number density (7–9 $\times$ $10^7/cm^3$) pseudoglow discharge plasma, which is typical for dielectric-barrier discharges at atmospheric pressure.[3,8–12] Electron-neutral collision is dominant as the ionization fraction is low, and thus the plasma conductivity is determined by both electron-neutral and electron-ion collisions with much less contribution from electron-ion collisions.[12–15] The discharge generates electrons, ions, excited atoms, and molecules, as well as UV radiation. Careful addition of other gases into the helium flow prevents development of streamers and generates a very uniform glow discharge plasma between the two electrodes inside the treatment active volume.[3,8–12] Gas inlet is provided from the side of the chamber and is circulated via multiple inner inlets to ensure uniformity of gas distribution inside the test cell. An exhaust canopy is installed on the top of the main chamber.

The device is capable of batch treatment of films and fabric pieces using the inner test cell. Samples are placed within the test cell on a nylon grid, which is suspended in the middle of the test cell to allow for complete and uniform plasma exposure on all sides. The device is also capable of continuous operation using the roller feed system for large fabric rolls or continuous filaments and yarns. Figure 1 shows a schematic drawing of the device in which the substrate represents batch treatment inside the test cell, and the roller system represents continuous treatment of fabrics and yarns.[8,9,12]

Figure 2 shows a simplified electric circuit diagram of the device, in which C_T and R are coupling capacitors and resistors, and C represents the two electrodes in the capacitively-coupled mode.[8,9,12] The step-up transformers are at 180° out of phase, and the HVP is the locations of the capacitively-coupled compensated high voltage probe (Tektronix™ Model P6015A) for voltage measurements. The discharge current flowing through the plasma is measured by a current transformer with a current-

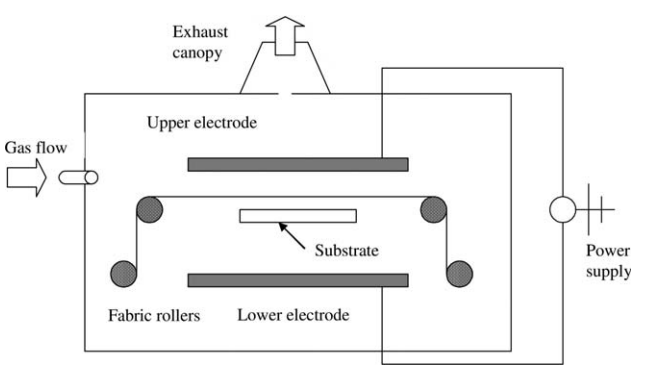

Figure 1 Schematic drawing of the atmospheric pressure plasma device (NCAPS).

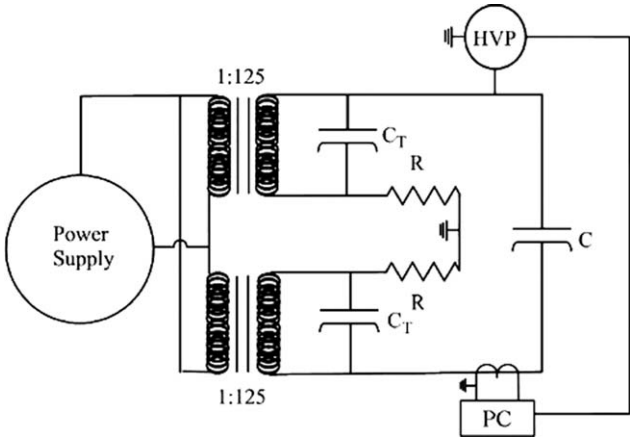

Figure 2 Schematic electrical circuit diagram of the atmospheric plasma device (NCAPS).

voltage ratio of 1 : 1 (Pearson Electronics ™ Current Monitor Model 2100). Both the high voltage probe and the Pearson coil are connected to a National Instruments PCI-6221 data acquisition board (PC).

In this study all samples were exposed to plasma using the test cell. For all test series the operating frequency was fixed to 5 kHz, and the electrode gap was adjusted to 3.8 cm during all experiments.

Materials

PET films (Mylar® A) with a thickness of 300 μm were supplied by DuPont Tejin Films™. The films were cut into samples of 9 cm × 10.5 cm size. Prior to plasma exposure, the samples were washed with an acetone solution for 3 min and dried at ambient pressure. The PET samples were exposed to atmospheric plasma created with the following working gases.

- Helium (10 L_{He}/min)
- Helium (10 L_{He}/min) + 1 vol % oxygen
- Helium (10 L_{He}/min) + 1 vol % tetrafluoromethane
- Helium (10 L_{He}/min) + 1 vol % oxygen + 1 vol % tetrafluoromethane

The exposure time varied between 0.5 and 5 min in 30-s intervals. Electrical and thermal data were collected in the plasma during surface treatment of the PET films and were recorded via a National Instruments LabView® interface package. To identify correlations between plasma variation without and during the treatment of PET, three plasma measurements for each type of working gas without PET treatment were conducted and the average of the measured plasma parameters (plasma impedance, electron number density) was calculated for every gas type.

Characterization techniques

Computer-based control software

The NCAPS facility has been interfaced with the LabVIEW® package with in-house built-in mathematical solver to provide real-time electron number density, as well as real time monitoring of the plasma gas ambient temperature and gas flow rates. To optimize the performance of the atmospheric pressure plasma device, and to characterize the plasma, the diagnostics were interfaced with computer-based instrument control software. For this purpose the measurement and controlling software LabVIEW® 7.1 (National Instruments, Austin, USA) was used to create adequate interface and control panel for operating parameters and display of plasma parameters from the model solver.

To visualize the measured voltage and current on the computer, the LabVIEW® front panel was designed similar to an oscilloscope. Voltage and current are displayed by a waveform graph and used for further calculations of plasma impedance and electron density. The measured voltage and current are periodical, nonsinusoidal waveforms, hence, to calculate the time-dependent discharge impedance, or the impedance during a specific time domain, it is important to define a characteristic cycle mean value of such alternating signals. The interface calculates the cycle time and space averaged values root mean square (RMS) of voltage and current for each loop's iteration. Figure 3 shows the display and control panel of the atmospheric plasma device on which voltage and current waveforms are displayed in real time, and their RMS numerical values are displayed on the bottom boxes, also in real time, along with the RMS impedance, ambient temperature, electron-neutral collision frequency, and electron kinetic temperature and number density.

The impedance is calculated from the RMS voltage and current $Z_{RMS} = (V_{RMS}/I_{RMS})$. Assuming the entire discharge to be equivalent to a plasma-filled capacitor and using the homogeneous plasma model, the complex impedance of bulk plasma of a thickness d and cross-sectional area A is given by $Z_P = 1/(j\omega\ \varepsilon_0\ \varepsilon_P\ A/d)$, where ε_o is the permittivity of free space and ε_p is the relative permittivity of the plasma (plasma dielectric constant).[13,14]

Since the thickness of the bulk plasma (d) is much greater than the time averaged thickness of the plasma sheaths (s) and $d + 2s = l$, where l is the gap of the capacitor, it is assumed that the thickness of the plasma $d \approx l$. The complex plasma dielectric constant is given by $\varepsilon_P = 1 - [\omega_{pe}^2/(\omega^2 - j\omega\ \nu_{en})]$ where ω_{pe} is the electron plasma frequency and is given by $\omega_{pe} = (n_e\ e^2/m_e\ \varepsilon_o)^{1/2}$, where n_e is the electron number density, e is the unit charge, m_e is the

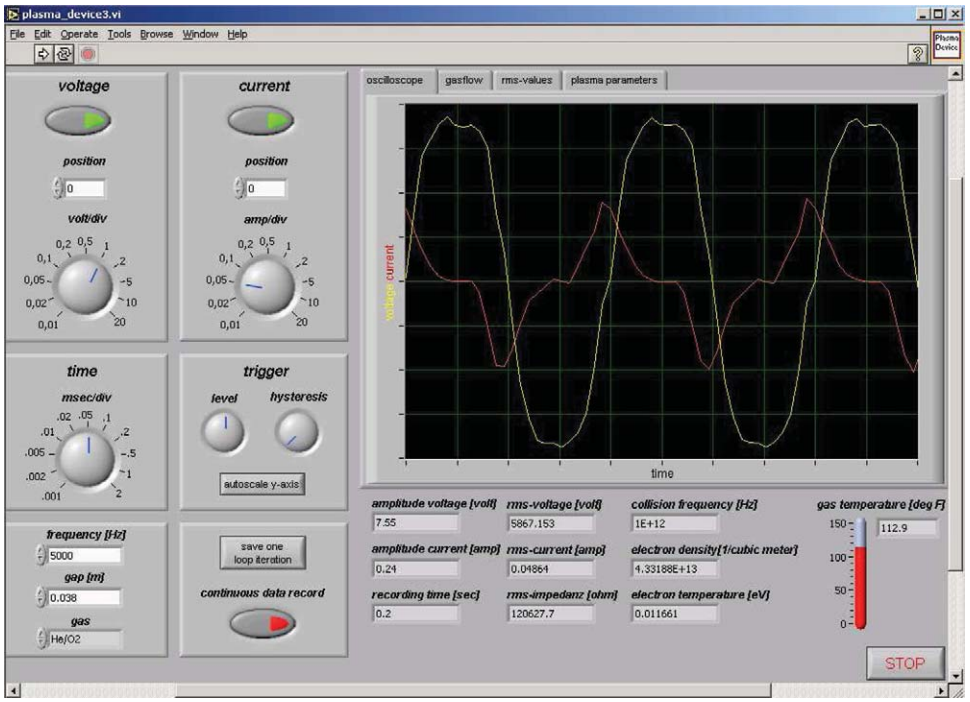

Figure 3 Display and control panel of the atmospheric plasma device showing the continuous display of the discharge voltage and current waveforms and the numerical values of plasma parameters. [Color figure can be viewed in the online issue, which is available at wileyonlinelibrary.com.]

electron mass; ν_{en} is the electron neutral collision frequency and ω is the operating angular frequency of the power supply. The sinusoidal current that flows through the plasma bulk can be described in complex notation as $I_{rf}(t) = \mathrm{Re}\ \tilde{I}_{rf}\, e^{j\omega t}$ and the voltage across the plasma is given by $V_p(t) = \mathrm{Re}\ \tilde{V}_p\, e^{j\omega t}$, where "Re" represents the real values and hence the plasma admittance is determined from the measured amplitudes of the current and voltage $Y_p = \tilde{I}_{rf}/\tilde{V}_p$.

Substituting for the plasma dielectric constant ε_P and the electron plasma frequency ω_{pe} in the plasma admittance equation and solving for the electron number density one obtains $n_e = (\tilde{I}_{rf}/\tilde{V}_p)\ (m_e\, d/e^2\, A)\ [(\omega^2 + \nu_{en}^2)/\nu_{en}]$. A key parameter in this equation is the electron-neutral collision frequency ν_{en}, which is sensitive to changes in plasma composition. The electron neutral collision frequency is given by $\nu_{en} = n_n\, v_e\, \sigma$, where n_n is the number of neutral atoms, v_e is the electron velocity and σ is the collision cross section. The number of neutral atoms can be obtained from the ideal gas law $n_n = P/kT$ with parameters taken at the gas inlet to the reaction chamber in which P is the pressure and T is the gas ambient temperature. The electron velocity is taken to be the average thermal velocity $\overline{v}_e = (8kT_e/\pi\, m_e)^{1/2}$ and the collision cross section is determined from the solid sphere model. Hence, the electron-neutral collision frequency is given by $\nu_{en} = \sigma\ (P/kT)\ (8kT_e/\pi\, m_e)^{1/2}$. Most dielectric barier discharge plasmas have electron temperatures between 0.5 and 1.2 eV as commonly reported, as well as data obtained from optical emission spectra.[8,10,14–16] The average electron-neutral collision frequency for helium at 1.0 atm is $\sim 7 \times 10^{11}$ Hz.[12–14,17] For simplicity, this frequency is taken into the equation of electron number density as an average value for helium discharge even with the addition of small fractions (1 and 2%) of other gases. The built-in solver provides real time monitoring of plasma electron number density, as well as continuous monitoring of the ambient gas temperature via a Teflon-coated thermocouple interfaced with the LabView instrument control package.

Weight changes

Each sample was weighed instantaneously before (W_0) and after plasma treatment (W_1), to determine weight gain or loss, using an Explorer® microbalance with an accuracy of ±100 μg. The percent weight change calculated as *Weight change* % = $(W_1 - W_0) \times 100/W_0$ was then plotted versus the exposure time.

Contact angle measurement

Contact angle measurement was realized at room temperature with a goniometer (Model A-100 by

Ramé-Hart) by the sessile drop technique using a 1 μL deionized water droplet on the PET film. The water was introduced on the sample surface by a microsyringe, afterward the contact angle was measured by a telescope equipped with a goniometer eyepiece. The contact angle was measured in five different places to determine hydrophobicity. The average contact angle was then plotted versus exposure time for all four plasma gas mixtures. Contact angle measurements were all conducted 24 h after plasma treatment.

Dynamic mechanical analysis

The tensile modulus was determined by dynamic mechanical analysis (DMA) using a DMA Q800 (TA Instruments). The tests were conducted isothermally at 25°C inside the furnace of the DMA device. The films were exposed to oscillating strain at constant amplitude with a stepwise linear frequency increase from 1 to 100 Hz in 25 steps. Since the PET films are nonisotropic materials, all Young's moduli were measured in machine direction (MD). The average of the obtained complex modulus values for every frequency step was calculated, and the complex modulus change plotted over exposure time. The complex modulus (*cmc*) percent change was obtained from $cmc\ \% = (E_1 - E_0) \times 100/E_0$, where E_0 is the original modulus and E_1 is the modulus after plasma exposure.

RESULTS AND DISCUSSION

Plasma ambient temperature

The plasma gas ambient temperature is continuously monitored via a Teflon-coated thermocouple immersed in the plasma and is interfaced with the LabVIEW instrument control; the ambient temperature is displayed on the front display and control panel. The ambient gas temperature inside the test cell increases by 9–10°F (5.0–5.6°C) for most gases within 30 s and increases by 20–24°F (11.1–13.4°C) after 300 s, except for Helium + 1%O_2 + 1%CF_4 it increases by 15°F (8.3°C) in 30 s and by 33°F (18.3°C) after 300 s. Table I shows the increase in ambient temperature for all plasma gas compositions. Comparisons of gas temperatures of helium, He/O_2 and He/CF_4 discharges show that the increase in the ambient temperature is small; the case of He/O_2/CF_4 has a slightly higher temperature increase. This effect is explainable with the inclusion of the energetic gases O_2 and CF_4 to the seed gas, which allows for generation of more reactive species that are chemically reactive and causes temperature increase. Because of generation of more reactive species, molecular collisions are increasing inside the gas mixture and lead to an increase in the ambient temperature. The temperature increase for all used gases indicates that the maximum temperature increase is below the glass transition temperature for PET (69°C, 156.2°F), which is important for nonthermal plasma treatment of PET. Accordingly, no thermal effects are imposed on the PET films during plasma treatment in the NCAPS device.

Plasma impedance

Plasma generation in a capacitively-coupled dielectric barrier discharge affects the overall impedance of the system due to electron collisional processes inside the plasma and the formation of ions, excited species, and radicals; consequently the change in the plasma gas composition will change the total impedance. The plasma impedance for pure helium discharge has a slight decrease from 116.5 to 115 kΩ in the first 30 s then remains almost unchanged over time. Impedance increases from 114 to 115 kΩ over 300 s for He/O_2, from 113 to 116 kΩ for He/CF_4, and from 112 to 117 kΩ for He/O_2/CF_4. The observed increase in the impedance of He/O_2, He/CF_4, and He/O_2/CF_4 is due to formation of additional ionic and radical species. The increase can be explained from the plasma impedance equation when considering the device as a capacitor filled with plasma. The real value of the plasma impedance $Z_P = (d/\omega\ \varepsilon_0\ \varepsilon_P\ A)$ is a function of the plasma dielectric constant ε_p, which is a function of the electron plasma frequency ω_{pe} and the electron neutral collision frequency ν_{en}. The change in plasma composition changes both frequencies as a result of different ionization fractions, changes in the electron number density, and the collision of electrons with

TABLE I
Ambient Temperature Inside the Plasma Test Cell After 30 and 300 s

Plasma gas	Initial temperature (°F)	After 30 s		After 300 s	
		Temperature (°F)	ΔT (°F)	Temperature (°F)	ΔT (°F)
Helium	83 (28.3°C)	92 (33.3°C)	9 (5.0°C)	103 (39.4°C)	20 (11.1°C)
Helium + 1%O_2	83 (28.3°C)	93 (33.9°C)	10 (5.6°C)	107 (41.7°C)	24 (13.4°C)
Helium + 1%CF_4	82 (27.8°C)	91 (32.8°C)	9 (5.0°C)	102 (38.9°C)	20 (11.1°C)
Helium + 1%O_2 + 1%CF_4	80 (26.7°C)	95 (35.0°C)	15 (8.3°C)	113 (45.0°C)	33 (18.3°C)

additionally generated species either in ionic or excited forms.

The RMS impedance of He/O_2 discharge increases slightly over 5-min operating time, which is attributed to the change in the nature of the plasma due to formation of oxygen ions O^+, excited oxygen atoms O^*, and possible negative oxygen ions O^-. For He/CF_4 discharge the increase of RMS impedance over operating time is more appreciable, however, it is similar to the oxygen case in that when other species are generated in the plasma they affect the collision frequency which in turn affects the plasma admittance. For CF_4 these additional species could be F, F^+, $(CF_3)^+$, CF_2, and $(CF_2)^+$. The same reasoning applies to the $He/O_2/CF_4$ discharge. Because of the formation of additional species and alterations in the collision frequency, the plasma dielectric constant changes and the impedance increases. The effect is most distinctive for $He/O_2/CF_4$ discharge since more reactive gases are added to the seed gas and more collisional processes takes place in the discharge.

The plasma impedance drops with the inclusion of PET samples in the test cell. For the pure helium discharge, the inclusion of the PET dropped the impedance to 107.5 kΩ, and a slight drop to 114 kΩ for the He/O_2 discharge. The impedance for He/CF_4 and $He/O_2/CF_4$ with PET dropped to 110k Ω in both cases. The impedance drop, in all cases, is attributed to the increased electron collisions with species entering the plasma from the etched surface of the PET samples followed by recombination and reduction in the charged particles population.

This can be explained from the plasma impedance $Z_p = (n_e\ e^2A/m_e\ d)[\nu_{en}/(\omega^2 + \nu_{en}^2)]$, which is a function of the operating frequency ω, the electron-neutral collision frequency ν_{en}, and the electron number density n_e. Atmospheric dielectric barrier discharge plasmas are generated at low frequency in the kHz range (1–12 kHz) and the electron neutral collision frequency for most gases at atmospheric pressure is in the range of 10^{11} Hz,[13,16] consequently the impedance equation can be approximated to $Z_p \cong (e^2A/m_e\ d)(n_e/\nu_{en})$. The electron number density $n_e = \sum_{k=1}^{g} (n_i)_k$ is the sum of all ionic populations in the plasma from only a single species $k = 1$ to any arbitrary number of species g, and hence the plasma is quasi-neutral. The ratio between the electron number density and the electron neutral collision frequency n_e/ν_{en} determines the behavior of the plasma impedance. The impedance drops as a result of increased collisional frequency with etched species and reduction in electron populations due to recombination with ionic species and cooling of the plasma. The reduction in the electron number density is discussed in the following section.

Electron number density

The obtained electron density for the NCAPS device without PET exposure is always in the range of 7.5 $\times$ 10^7 cm^{-3} to 8.5 $\times$ 10^7 $cm^{-3}$for all gas types. For Helium, He/O_2, and $He/O_2/CF_4$ discharge the electron density remains nearly constant over 5-min operating time, as shown in Figure 4. As opposed to pure Helium discharge the electron density for He/O_2 and $He/O_2/CF_4$ discharges slightly increased, which is attributed to the addition of a reactive gases and the increased ionization of plasma species. Unexpected is the behavior of electron density for He/CF_4 discharge. As shown in Figure 4 the electron density is decreasing continuously over operating time. The decrease in electron population may be attributed to the strong recombination effects arising from recombination of molecular $(CF_3)^+$ and $(CF_2)^+$ with electrons. While this behavior is not seen in the $He/O_2/CF_4$ case where CF_4 is included, however, the presence of oxygen in the gas mixture may produce negative and molecular oxygen ions that increases the ionic population and balances recombination with fluorocarbon species.

The electron number density for all operating gases during PET exposure with plasma shows a constant behavior after initial fluctuations indicating a stable plasma condition during sample treatment. There is always a reduction in the electron number density for all tested plasma gases. To visualize the effect of PET ablation on the electron density due to etching, a comparison between electron density with and without PET by subtraction of the particular curves was performed as shown in Figures 5 through 8 for helium, He/O_2, He/CF_4, and $He/O_2/CF_4$, respectively. Plasma interaction with PET substrate lowers the electron number density due to increased number of etched particulates from PET, which re-attach to free electrons inside the plasma. When PET is etched, the radicals are in an excited

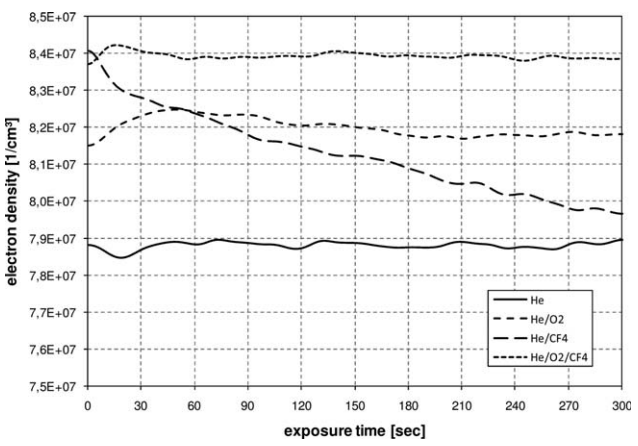

Figure 4 Electron number density without PET sample in the plasma.

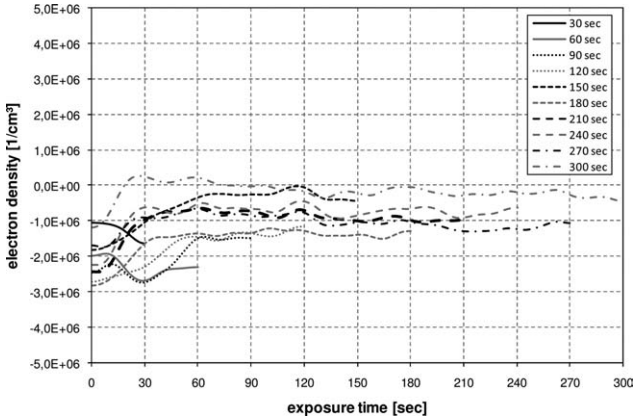

Figure 5 Net reductions in electron number density with PET sample in the Helium plasma.

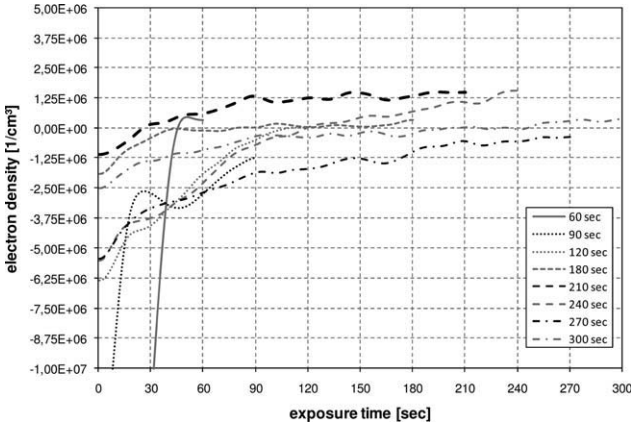

Figure 7 Net reductions in electron number density with PET sample in the He/CF_4 plasma.

state and are able to capture electrons to neutralize themselves, which, in combination with ionic species recombining with electrons to formulate neutrals, causes a reduction in electron number density with inclusion of the PET samples in the plasma. Investigation of the helium discharge case, Figure 5, shows an average reduction in the electron number density of about $1.25 \times 10^6/cm^3$ when PET is in the plasma. The extended exposure time did not change the electron number density as most etched species are becoming part of the plasma and ionized during the extended operation cycle. The He/O_2 case, Figure 6, has an average reduction of about $5 \times 10^6/cm^3$, which is higher than that of pure helium, and is attributed to the added collisional processes with oxygen ionic and excited species.

The He/CF_4 case, Figure 7, has a different behavior, the electron number density shows sudden drops to close to a net reduction of $1.0 \times 10^7/cm^3$ in the 60 and 90-s exposure times then less reduction for extended PET exposure times. It appears that any strong recombination effects are within the shorter exposure times but extended exposure produces more ionized species from the ablated material from the PET surface. The effect is similar in the case of $He/O_2/CF_4$, Figure 8, where strong reductions take place in the shorter exposure time, but not for extended exposure due to additional ionization of etched species entering the plasma stream.

In general, the electron density is in the range 7.5×10^7 cm^{-3} to 8.5×10^7 cm^{-3}, which is in good agreement with published data for similar devices, as well as data obtained by other researchers on the NCAPS device using optical emission spectra and other measuring techniques.[2,8,11,12,18,19]

Surface etching of PET in plasma treatment has been investigated in previous studies on the NCAPS device,[9,20] which showed that percent crystallinity increases as a result of selective amorphous etching and that the rate of etching is also related to the degree of solubility.[9] Reactions between plasma and PET surface may generate several chemical by-products such as CO, CO_2, H_2O, OH, H^*, H_2, and radicals,[20] all can adversely affect the collisional processes in the plasma.[20] The surface condition of the PET changes as a result of the plasma treatment, as

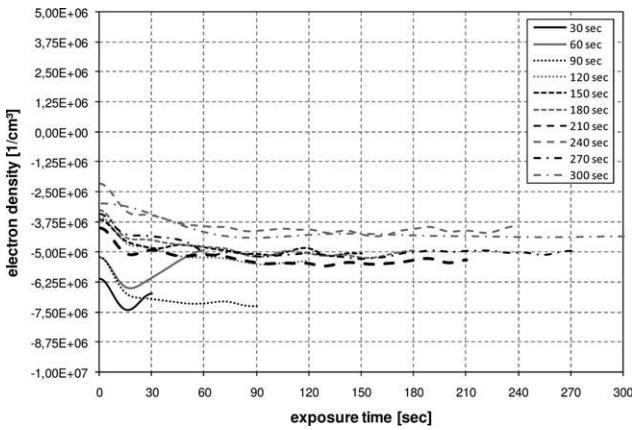

Figure 6 Net reductions in electron number density with PET sample in the He/O_2 plasma.

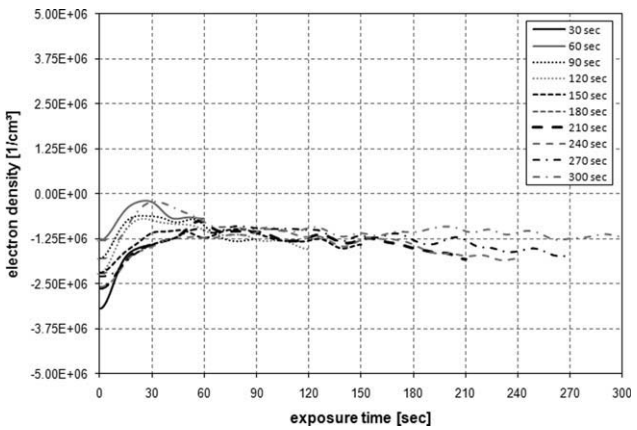

Figure 8 Net reductions in electron number density with PET sample in the $He/O_2/CF_4$ plasma.

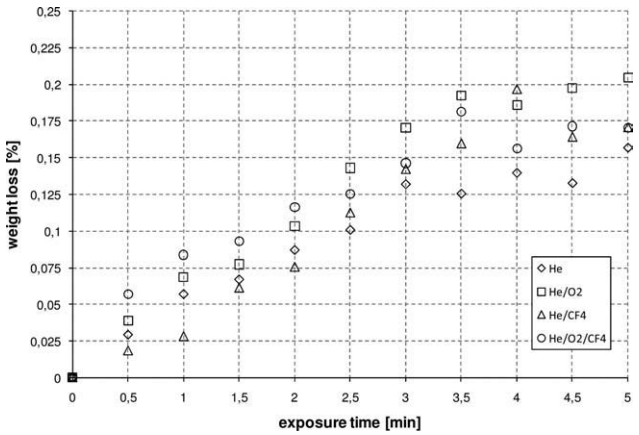

Figure 9 Weight loss of plasma treated PET films versus exposure time.

has been shown by Hwang et al.[20] in which the XPS and AFM indicated surface changes in terms of roughness, chemical composition, crosslinking, and redeposition.[20] It was also evident that the population of etched particles increases over the entire exposure time, mixes with the plasma, and hence changes the plasma composition.[20]

Weight loss

Weight loss measurements of plasma treated PET films indicate that etching takes place for all operating gases. Figure 9 illustrates the weight loss in percent as a function of exposure time for He, He/O_2, He/CF_4, and $He/O_2/CF_4$ discharges. It is obvious that surface etching starts immediately when exposing the films to the plasma and is increasing with exposure time. It is worthy to mention that the electron number density prior to immersing the substrate is of higher value then levels off with extended exposure time. This indicates a higher number of ionic species at the beginning of the discharge, as plasma is quasi-neutral, and the number reduces with increased exposure time; as reaction with ions takes place more etching is expected as seen from Figure 9. For helium discharge, maximum weight loss is reached after 3 min, for He/O_2 after 3.5 min, for $He/O_2/CF_4$ discharge, and after 4 min for the He/CF_4 discharge. After reaching the maximum, weight loss remains approximately constant for all treatments. This trend indicates that initially etching effects are dominant for all gas types until saturation of PET volatiles inside the plasma cell is reached, then etching and re-deposition effects reach equilibrium.

The comparison of the different curves shows that the presence of oxygen in the discharge provides a higher etching rate when compared to etching in pure helium plasma. Typically, helium is not considered as an etching gas however, helium ions can sputter the substrate surface.[21] Oxygen ions in the plasma lead to additional physical and chemical etching processes and therefore weight loss is increased for He/O_2 discharge. As shown in Figure 9, addition of CF_4 to a helium discharge also increases etching rates. One reason is that CF_4 is easily dissociated, which results in a relatively high density of free fluorine. This creates plasma with highly reactive fluorine and higher sputtering ability.[22] Recapitulating, it can be noted that etching takes place for all four gas types, whereas the He/O_2 gas mixture proved to be the most effective etching gas. Weight loss results indicate that generated ions and active plasma species in the plasma gas, and dissociated molecules from the etched surface, recombine with electrons and results in reduction of the electron number density as has been shown in the preceding section. Upon recombination, these newly formed atoms and molecules in their excited state continue to etch the surface and increase ablation over time; hence the weight loss increases with increased exposure time. The previous study on plasma treatment of PET using He/O_2 gas by Hwang et al. demonstrated that etching and redeposition are occurring simultaneously, and the weight loss can be divided into loss at amorphous and crystalline regions.[20]

Contact angle measurement

Wettability of plasma treated PET films was estimated by contact angle measurement. Figure 10 shows the contact angle as a function of exposure time for the four different working gases. For all gas types, contact angle of PET films is decreased after plasma treatment, thus wettability is increased. For He and $He/O_2/CF_4$ discharge the contact angle drops rapidly until 1 min exposure time and then levels off, and levels off at 2.5 min for the He/O_2

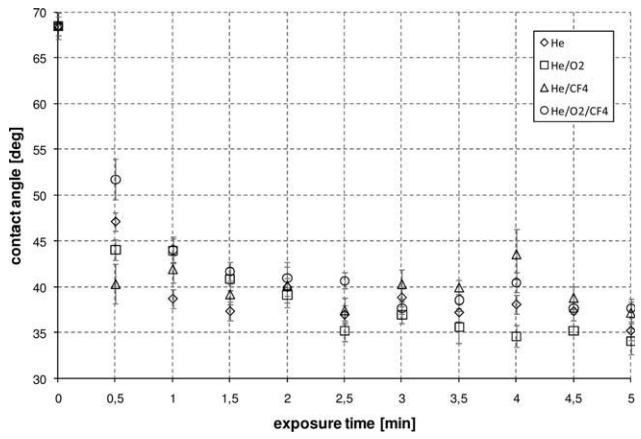

Figure 10 Contact angle of plasma treated PET film versus exposure time.

discharge. For He/CF_4 discharge the contact angle drops most rapidly in the beginning but already starts leveling off at 30 s exposure time.

After reaching the limiting values, the contact angle values for He/O_2 discharge are lower than that for pure He discharge. Thus He/O_2 gas treatment leads to higher wettability than pure Helium gas treatment. Since He/O_2 gas has more oxygen content, it is possible that more hydrophilic functional groups can be created through more interactions with molecules on PET film surface.

While the measured contact angles of PET after treatment with He/CF_4 discharge (after 30-s exposure time) are higher than that of pure helium discharge, the overall plasma effect is an increase of hydrophilicity. There appears to be little effect of incorporation of F-atoms and —CHF, —CF_2—, as well as —CF_3 groups on the PET surface during plasma treatment with fluorocarbon gases.[23]

The trend for electron number density versus exposure time is similar to that of the contact angle. The relation between the contact angle and the decrease in the electron number density may be attributed to the electron impact on reactive plasma gases, followed by dissociation of gaseous species into ions and electrons. The ions bombard the surface and form reactive surface groups that increase hydrophilicity, but subsequently consume the electrons in recombination processes. It is also possible that surface etching contributes to the reaction between surface etched species and electrons, as well as reactions with formed radicals. The previous study on plasma treatment of PET indicated etching and redeposition occurring simultaneously,[20] however, etching may be predominant in the case of He/CF_4. The AFM micrographs, as shown in our previous study, showed higher surface roughness in the He/O_2 treated PET.[20] Also, XPS analysis revealed distinctive changes in chemical composition and formation of new functional groups.[20]

Cross linking and chain-scission

To characterize effects of crosslinking and chain-scission, the Young modulus of PET films after plasma exposure was measured using dynamic mechanical analysis (DMA). The percent change in complex modulus was calculated and plotted versus exposure time. Crosslinking and chain scission lead to changes in the physical and mechanical properties of polymers. If chain scission is dominant during plasma treatment, a decrease in mechanical properties such as Young's modulus will occur. Crosslinking, on the other hand, leads to increases in mechanical properties including hardness, tensile strength and Young's modulus.

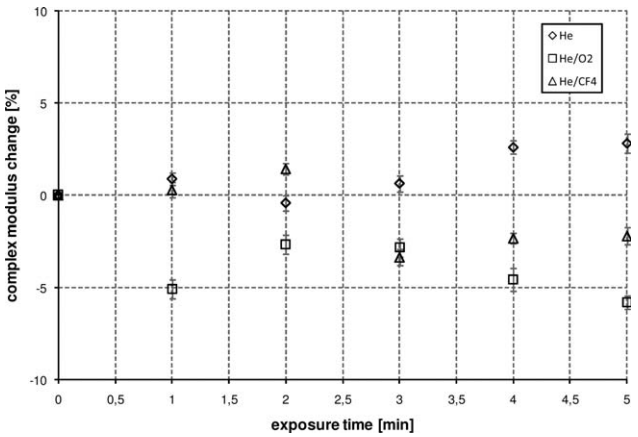

Figure 11 Complex modulus change of plasma treated PET films versus exposure time.

As displayed in Figure 11, the Young's modulus for PET films increases with exposure time for He discharge. After 5 min the modulus is enhanced by $\sim$ 2.8%. This corroborates results of a previous study on PET films, which showed similar tensile strength enhancement of PET films by helium containing plasmas.[24] In these studies, atmospheric plasmas with high helium percentages (as opposed to mixtures of He with reactive gases, e.g., oxygen) were found to have increases in C—C bonds after exposures of 1 min or longer. This is indicative of crosslinking due to an abundance of UV radiation from ion neutralization, Auger deexcitation, and Penning ionization.[20] Figure 11 shows a slight decrease of Young's moduli for He/O_2 and He/CF_4 discharges. This can be attributed to etching effects that are more pronounced for mixtures of helium and reactive gases than for pure He plasmas. These results indicate that chain-scission of the substrate surface, rather than crosslinking, is the dominant factor in determination of mechanical properties in these plasmas. Unfortunately, all of the $He/O_2/CF_4$ samples were broken in the course of DMA testing, and therefore, modulus data is unavailable for these samples.

CONCLUSIONS

Plasma electron number density was obtained in real time to relate the change in the electron number density to other measurements and to further understand the mechanisms of plasma–surface interactions. A mathematical solver based on a model assuming the plasma device acting as a plasma-filled capacitor was built inside the LabView instrumentation interface package. The program automatically solves the impedance equation based on the measured discharge voltage and current, and continuously displays the number density on the emulated instrument control panel.

The ambient gas temperature increased for all tested plasma gas mixtures with maximum increase of $\sim 5^{\circ}C$ in 30 s for all gases except for $He/O_2/CF_4$ mixture, where the increase was 8.3°C. After 300 s, the maximum increase was $\sim$ 11–13°C for all gasses except for $He/O_2/CF_4$ mixture where the increase was 18.3°C. Hence, temperature increase in all cases is below the glass transition temperature for PET, indicating nonthermal plasma treatment of PET in the NCAPS device.

The calculations of electron density using the built-in plasma model are in the range 7.5×10^7 cm^{-3} to 8.5×10^7 cm^{-3} and are in good agreement with published data for similar devices, as well as data obtained by other researchers on the device using optical emission spectra and other measuring techniques. A decrease in the electron density during the treatment of PET films was observed, which relates to etching of the PET films followed by reattachment and recombination. The drop in the electron number density follows the drop in the plasma impedance, which results from increased collisional frequency with etched species and the reduction in the electron population due to recombination with ionic species and cooling of the plasma.

Surface and bulk analyses of the plasma treated PET films indicate etching effects on the substrate surface for all gas types, with more etching of the surface with the addition of reactive gases such as oxygen and CF_4. However, the He/O_2 gas mixture has shown the highest etching effect, which is in good agreement with previous work on plasma treatment of PET on the NCAPS device.[9] As a result of the closed chamber geometry, etching continued until saturation and then reached equilibrium with re-deposition from the plasma onto the substrate.

Contact angle measurements showed that wettability of PET surfaces increases after plasma exposure for all four operating gases, where He/O_2 caused the highest contact angle prior to decrease here and He/CF_4 the least. This confirms that the primary effect of the CF_4 gas is etching rather than fluorination; however, fluorine content may be responsible for the relatively higher contact angles as compared to the samples treated in the other plasma gases.

Measurements of Young's modulus with dynamic mechanical analysis (DMA) showed an increase of the modulus of PET after treatment with helium discharge, whereas the modulus decreased slightly after treatment with oxygen and tetrafluoromethane containing gases. The enhanced Young's modulus for helium discharge confirmed previous studies since helium is known as an effective crosslinking gas, which improves mechanical properties of polymer materials. The degradation of the modulus after plasma exposure to oxygen and tetrafluromethane gases is most likely a result of increased etching and chain-scission.

The authors are thankful to Dr. Carrie Cornelius for her help in running the experiment during the course of this study.

References

1. Bronzino, J. D. The Biomedical Engineering Handbook: Biomedical Engineering Fundamentals; Taylor & Francis: New York, 2006.
2. Chu, P. K.; Chen, J. Y.; Wang, L. P.; Huang, N. J Mater Sci Eng 2002, R36, 134.
3. Jensen, N.; Lindblad, B.; Bergavist, D. Eur Surg Res 1996, 28, 49.
4. Foxall, T. L.; Auger, K. R.; Callow, A. D.; Libby, P. J Surg Res 1986, 41, 158.
5. Dee, K. C.; Andersen, T. T.; Bizios, R. Tissue Eng 1995, 1, 135.
6. van Wachem, P. B.; Vreriks, C. M.; Beugeling, T.; Feijen, J.; Bantjes, A.; Detmers, J. P.; van Aken, W. G. J Biomed Mater Res 1987, 21, 701.
7. Ertel, S. I.; Ratner, B. D.; Horbett, T. A. J Biomed Mater Res 1990, 24, 1637.
8. Bures, B. L.; Donohue, K. V.; Roe, R. M.; Bourham, M. A. IEEE Trans Plasma Sci 2005, 33, 290.
9. Matthews, S. R.; Hwang, Y. J.; McCord, M. G.; Bourham, M. A. J App Polym Sci 2004, 94, 2383.
10. Roth, J. R.; Sherman, D. M.; Gadri, R. B.; Karakaya, F.; Chen, Z.; Monti, T. C.; Kelly-Winterberg, K.; Tsai, P. Y. IEEEE Trans Plasma Sci 2000, 28, 56.
11. Laroussi, M.; Alexeff, I.; Richardson, J. P.; Dyer, F. F. IEEE Trans Plasma Sci 2002, 30, 158.
12. Bures, B. L. Rapid Mortality of Pest Arthropods by Direct Exposure to Dielectric Barrier Discharge 2004, Ph.D. dissertation, NCSU, USA.
13. Liebrman, M. A.; Lichtenberg, A. J. Principles of Plasma Discharges and Materials Processing, 2nd ed.; Wiley: Hoboken, New Jersey, 2005.
14. Roth, J. R. Industrial Plasma Engineering: Principles; Institute of Physics Publishing: Bristol and Philadelphia, 1995; Vol. 1.
15. Park, J.; Henins, I.; Herrmann, H. W.; Selwyn, G. S. Phys Plasmas 2000, 7, 3141.
16. Ricard, A.; Décomps, Ph.; Massines, F. Surface Coat Technol 1999, 112, 1.
17. Roth, J. R. Industrial Plasma Engineering: Applications to Nonthermal Plasma Processing; Institute of Physics Publishing: Bristol and Philadelphia, 2001; Vol. 2.
18. Bures, B. L.; Donohue, K. V.; Roe, R. M.; Bourham, M. A. IEEE Trans Plasma Sci 2006, 34, 55.
19. Donohue, K. V.; Bures, B. L.; Bourham, M. A.; Roe, R. M. J Economic Entomol 2006, 99, 38.
20. Hwang, Y. J.; Matthews, S.; McCord, M.; Bourham, M. J Electrochemic Soc 2004, 151, C495.
21. Clark, D.; Wilson, R. J Polym Sci Polym Chem Ed 1983, 21, 837.
22. Hippler, R.; Pfau, S.; Schmidt, M.; Schoenbachm, K. H. Low Temperature Plasma Physics: Fundamental Aspects and Applications; Wiley-VCH Verlag: Berlin, 2001.
23. Hyun, J. Plasma Surface Modification of Polymers, Characterization, Immobilization, and Simulation of Surface Dynamics, Raleigh, North Carolina State University, Department of Materials Science and Engineering, Dissertation, 1999.
24. Gurnett, D. A.; Bhattacharjee, A. Introduction to Plasma Physics: With Space and Laboratory Applications; Cambridge University Press, Cambridge UK, New York USA, 2005.